Polymer Journal (2017) 49, 649–654

www.nature.com/pj

ORIGINAL ARTICLE

Regioselective halogen–magnesium exchange reaction of a bithiophene derivative bearing methoxy and pyridine groups at the β-position and Kumada coupling polymerization

Koji Takagi, Ryo Kouchi and Junpei Kawai

We have previously reported the synthesis of a polythiophene derivative (P2′) bearing pyridine and methoxy groups at the β-position, but the halogen–magnesium exchange reaction of the monomer did not proceed in a regioselective manner and resulted in a twisted polymer conformation. In the present paper, the halogen–magnesium exchange reaction of 4-(5″-hexylpyridine-2″-yl)-3-methoxy-2-(5′-bromothiophene-2′-yl)-5-bromothiophene (M3) and its Kumada coupling polymerization and optoelectronic characterization were investigated. The reaction of M3 with *i*-PrMgCl·LiCl gave a Grignard monomer (GM3a) in 79% yield, with the halogen–magnesium exchange reaction occurring exclusively at the bromine atom neighboring the pyridine group. Reflux temperature was required for the Kumada coupling polymerization of GM3a using Ni(dppp)Cl_2 to proceed smoothly (72% conversion after 24 h) due to the sterically hindered monomer structure. On the other hand, the conversion of GM3a remained at 15% without the addition of LiCl. The number-average molecular weight of the tetrahydrofuran-soluble fraction of the regiocontrolled oligo(bithiophene) (P3′) was 2900 because of its poor solubility. Ultraviolet–visible and cyclic voltammogram measurements indicated that compared with P2′, P3′ has a more planar conformation, an increased highest occupied molecular orbital energy level and a narrower bandgap energy. A non-covalent S···O interaction was assumed to cause the planar conformation, which was supported by theoretical density functional theory calculations.
Polymer Journal (2017) **49,** 649–654; doi:10.1038/pj.2017.37; published online 19 July 2017

INTRODUCTION

Conjugated polymers have been attracting much attention in the past few decades because of their applications in organic photovoltaics, organic field-effect transistors and organic light-emitting diodes, and their lightweight and flexible properties over a large area. Because of the diverse molecular design for tuning their optoelectronic properties and their cost-effective film-forming characteristics, conjugated polymers can be used to create novel optoelectronic devices that are difficult to realize using silicon-based semiconductors. Poly (3-hexylthiophene) (P3HT), which is the most common conjugated polymer, can be synthesized in one step from commercially available monomers. In particular, regioregular head-to-tail P3HT has a significant advantage over the regiorandom variant owing to its high electronic conductivity, semicrystalline characteristics and wide absorption spectrum, which results in its superior performance in optoelectronic devices.[1,2] The synthesis of head-to-tail-P3HT was first reported by McCullough *et al.*[3,4] The regioselective metalation of 2-bromo-3-hexylthiophene using lithium diisopropylamide and subsequent treatment with $MgBr_2{\cdot}Et_2O$ or $ZnCl_2$ were performed at cryogenic temperatures, and then the nickel-catalyzed cross-coupling polymerization was conducted at room temperature. Later, the halogen–magnesium exchange reaction of 2,5-dibromo-3-hexylthiophene or 2-bromo-3-hexyl-5-iodothiophene with readily available Grignard reagents followed by the Kumada coupling polymerization under mild conditions were developed by McCullough *et al.*[3] and Yokozawa *et al.*[5–7] Thanks to the discovery of this innovative methodology, many thiophene-based conjugated polymers and materials can be obtained. Despite the many attractive features of head-to-tail P3HT, there are some problems to be resolved for its practical application, including the mismatched frontier energy levels between donor/acceptor materials and the relatively wide bandgap energy. The chemistry of side-chain engineering has been recently drawing considerable interest for manipulating the optoelectronic properties of polythiophene derivatives. In addition to the precision synthesis of linear head-to-tail P3HT, the modification of side chains[8–10] and the preparation of branched polythiophene derivatives[11–13] have been investigated by many research groups.

The introduction of aromatic rings at the β-position of thiophene can modify the electron density of the conjugated main chain to eventually influence the device performance.[14–18] We have synthesized a poly(3-pyridylthiophene) derivative (**P1** in Figure 1) from **M1**,[19,20] and the polymer molecular weight could roughly be controlled based

Life Science and Applied Chemistry, Graduate School of Engineering, Nagoya Institute of Technology, Nagoya, Japan
Correspondence: Professor K Takagi, Life Science and Applied Chemistry, Graduate School of Engineering, Nagoya Institute of Technology, Gokiso, Showa, Nagoya 466-8555, Japan.
E-mail: takagi.koji@nitech.ac.jp
Received 29 April 2017; revised 8 June 2017; accepted 8 June 2017; published online 19 July 2017

on the monomer/catalyst molar ratio, and high head-to-tail contents (89–99%) were attained. The energy levels of the highest occupied molecular orbital (HOMO) and the lowest unoccupied molecular orbital (LUMO) were successfully reduced by incorporating electron-deficient nitrogen heterocycles, but the polymer chains adopt a twisted conformation. Recently, to realize a planar conformation through intramolecular hydrogen bonding, we have reported the synthesis and characterization of a polythiophene derivative (**P2**) with pyridine and hydroxy groups at the β-position.[21] Unfortunately, in contrast to **M1**, the halogen–magnesium exchange reaction of **M2** did not proceed in a regioselective manner due to the competitive coordination of the pyridine nitrogen and ether oxygen,[22] resulting in a regiorandom structure and a twisted polymer conformation. In the present paper, new dibromobithiophene monomer **M3**, which features a thiophene ring appended adjacent to the methoxy group, was designed. In the halogen–magnesium exchange reaction of **M3**, because the chelate coordination of the pyridine nitrogen atom can guide the introduction of the chloromagnesium group at the carbon neighboring the pyridine ring, the Kumada coupling polymerization and subsequent polymer reaction would be expected to give regiocontrolled **P3** with a more planar conformation.

EXPERIMENTAL PROCEDURES

Materials

Isopropylmagnesium chloride solution (*i*-PrMgCl, 2.0 M in tetrahydrofuran (THF)), *i*-PrMgCl lithium chloride complex solution (*i*-PrMgCl·LiCl, 1.3 M in THF), and tetrakis(triphenylphosphine)palladium(0) ($Pd(PPh_3)_4$) were purchased from Sigma-Aldrich (Tokyo, Japan). 1,3-Bis(diphenylphosphinopropane)nickel(II) dichloride ($Ni(dppp)Cl_2$) was purchased from Tokyo Chemical Industry (Tokyo, Japan). Dry THF was purchased from Kanto Chemical (Tokyo, Japan). Other organic reagents and solvents were obtained from suppliers and used as received. 4-(5′-Hexylpyridine-2′-yl)-2-iodo-3-methoxythiophene was prepared as previously reported.[21]

Instruments

^{1}H and ^{13}C nuclear magnetic resonance (^{1}H-NMR and ^{13}C-NMR) spectra were measured on a Bruker (Billerica, MA, USA) AVANCE III HD 400 NMR spectrometer. Elemental analysis was performed on an Elementar (Hessen, Germany) Vario EL cube. Gel permeation chromatography analysis was carried out on a Shodex (Tokyo, Japan) GPC-104 system equipped with tandem LF-404 columns (THF as the eluent, flow rate = 1.0 ml min^{-1}, 40 °C) and an ultraviolet (UV) detector (Shimadzu SPP-20A, Kyoto, Japan). Number-average molecular weight (M_n) and molecular weight distribution (M_w/M_n) were determined based on a calibration curve made from standard polystyrene samples. UV–visible spectra were measured on a Shimadzu UV-1650 spectrophotometer in a 1 cm quartz cell. Electrochemical measurement was carried out on a BAS (Tokyo, Japan) 2323 bipotentiostat using a platinum disk working electrode, a platinum wire counter electrode and an Ag/Ag^+ reference electrode in a standard three-electrode cell. The polymer film cast onto a platinum disk was immersed in a nitrogen-saturated 0.1 M CH_3CN solution of tetrabutylammonium hexafluorophosphate (Bu_4NPF_6), and the voltage–current characteristics were obtained at a scan rate of 100 mV s^{-1}.

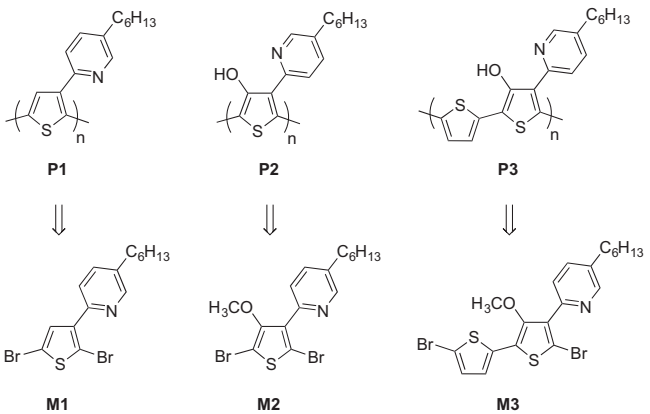

Figure 1 Structures of polythiophene derivatives and the corresponding monomers with a pyridine group at the β-position.

Monomer synthesis. *4-(5″-Hexylpyridine-2″-yl)-3-methoxy-2-(thiophene-2′-yl)thiophene (**1**).* A solution of 4-(5′-hexylpyridine-2′-yl)-2-iodo-3-methoxythiophene (3.40 g, 8.47 mmol), 2-tributylstannylthiophene (3.80 g, 10.2 mmol) and $Pd(PPh_3)_4$ (240 mg, 2.5 mol%) in toluene (70 ml) was heated to reflux for 3 days. After water was added, the aqueous phase was extracted with CH_2Cl_2. The combined organic phases were dried over $MgSO_4$, and solvents were removed using a rotary evaporator. Purification by SiO_2 chromatography (EtOAc:hexane = 1:12, R_f = 0.2) afforded 2.12 g (70% yield) of **1** as a yellow oil. ^{1}H-NMR (400 MHz, $CDCl_3$) δ p.p.m. 0.89 (t, J = 6.9 Hz, 3H), 1.27–1.39 (6H), 1.65 (m, 2H), 2.64 (t, J = 7.7 Hz, 2H), 3.69 (s, 3H), 7.05 (t, J = 4.3 Hz, 1H), 7.29 (d, J = 4.4 Hz, 2H), 7.56 (dd, J = 8.1, 2.2 Hz, 1H), 7.64 (s, 1H), 7.83 (d, J = 8.1 Hz, 1H) and 8.48 (d, J = 1.7 Hz, 1H). ^{13}C-NMR (100 MHz, $CDCl_3$) δ p.p.m. 14.1, 22.6, 28.9, 31.1, 31.7, 32.8, 60.8, 120.8, 121.5, 123.8, 124.8, 126.9, 134.4, 135.2, 136.5, 136.6, 149.8, 150.0 and 151.0.

*4-(5″-Hexylpyridine-2″-yl)-3-methoxy-2-(5′-bromothiophene-2′-yl)-5-bromothiophene (**M3**).* To a solution of **1** (2.00 g, 5.59 mmol) in THF (20 ml) and AcOH (20 ml) was added *N*-bromosuccinimide (1.99 g, 11.2 mmol) at 0 °C, and the mixture was stirred at room temperature overnight. After saturated $NaHCO_3$ solution and $Na_2S_2O_3$ solution were added, the aqueous phase was extracted with CH_2Cl_2. The combined organic phases were dried over $MgSO_4$m and solvents were removed using a rotary evaporator. Purification by SiO_2 chromatography (EtOAc:hexane = 1:12, R_f = 0.3) provided 0.78 g (27% yield) of **M3** as a yellow oil. ^{1}H-NMR (400 MHz, $CDCl_3$) δ p.p.m. 0.90 (t, J = 6.9 Hz, 3H), 1.30–1.42 (6H), 1.68 (m, 2H), 2.67 (t, J = 7.8 Hz, 2H), 3.49 (s, 3H), 6.91 (d, J = 3.9 Hz, 1H), 6.97 (d, J = 3.9 Hz, 1H), 7.46 (d, J = 7.8 Hz, 1H), 7.61 (dd, J = 8.1, 2.2 Hz, 1H) and 8.58 (s, 1H). ^{13}C-NMR (100 MHz, $CDCl_3$) δ p.p.m. 14.1, 22.6, 29.0, 31.0, 31.6, 32.9, 61.1, 109.2, 112.4, 122.4, 123.4, 124.3, 129.5, 134.9, 135.4, 136.3, 137.4, 149.2, 150.0 and 150.5. Anal Calcd for $C_{20}H_{21}Br_2NOS_2$: C, 46.61; H, 4.11; N, 2.72; and S, 12.44%. Found: C, 46.11; H, 4.20; N, 2.47; and S, 12.15%.

Halogen–magnesium exchange reaction (typical procedure). To a solution of **M3** (80 mg, 0.16 mmol) in THF (3 ml) was added *i*-PrMgCl·LiCl (1.3 M THF solution, 0.12 ml, 0.16 mmol) at 0 °C. After the reaction had been conducted for 1 h, 1 M HCl followed by saturated $NaHCO_3$ solution were added. The aqueous phase was extracted with CH_2Cl_2, and the combined organic phases were dried over $MgSO_4$. Solvents were removed using a rotary evaporator, and the crude product was purified by SiO_2 chromatography (CH_2Cl_2:hexane = 4:1, R_f = 0.36) to give 54 mg (79% yield) of a yellow oil. ^{1}H-NMR (400 MHz, $CDCl_3$) δ p.p.m. 0.89 (t, J = 6.9 Hz, 3H), 1.28–1.38 (6H), 1.65 (m, 2H), 2.63 (t, J = 7.7 Hz, 2H), 3.68 (s, 3H), 6.99 (2H), 7.56 (dd, J = 8.1, 1.9 Hz, 1H), 7.63 (s, 1H), 7.78 (d, J = 8.1 Hz, 1H) and 8.47 (d, J = 1.5 Hz, 1H).

Kumada coupling polymerization (typical procedure). After **M3** (150 mg, 0.29 mmol) was subjected to the halogen–magnesium exchange reaction as described above, a THF suspension of $Ni(dppp)Cl_2$ (3 mol%) was added in one portion, and the mixture was heated to reflux for 24 h. The polymerization was quenched by adding 1 M HCl, and then saturated $NaHCO_3$ solution was added. The organic phase was diluted with $CHCl_3$ and poured into hexane to obtain 41 mg (40% yield) of a deep purple solid. M_n = 2900 and M_w/M_n = 1.4 (THF-soluble fraction).

RESULTS AND DISCUSSION

Monomer synthesis and halogen–magnesium exchange reaction

Dibromobithiophene monomer **M3** was synthesized according to Scheme 1. The starting material 4-(5′-hexylpyridine-2′-yl)-2-iodo-3-

methoxythiophene was obtained in high yield via the regioselective iodination of 4-(5′-hexylpyridine-2′-yl)-3-methoxythiophene using I_2/PhI(OAc)$_2$ in THF/AcOH, as reported previously.[21] The Stille coupling reaction followed by bromination using conventional methods successfully provided **M3**. The structure and purity of **M3** were validated using NMR spectroscopy (Supplementary Figure S1) and elemental analysis. The halogen–magnesium exchange reaction of **M3** was initially carried out by adding *i*-PrMgCl·LiCl (the turbo-Grignard reagent) dropwise at 0 °C (Scheme 2). The reaction was quenched with 1 M HCl solution after 1 h, and the crude product was purified by SiO_2 column chromatography to obtain a yellow oil in 79% yield. Because all the proton signals of **M3b**, including H_b, should exhibit a multiplet splitting pattern, the isolated product was confirmed as **M3a**, and the singlet proton signal observed at 7.63 p.p.m. can be assigned to H_a (Supplementary Figure S2). In the ^{1}H-NMR spectrum of the crude mixture, the methoxy proton signals of **M3** and **M3a** are observed at 3.49 and 3.68 p.p.m., respectively (Figure 2). Similarly, the signals of the proton adjacent to the pyridine nitrogen are observed at 8.58 and 8.47 p.p.m. for **M3** and **M3a**, respectively. No proton signals corresponding to **M3b** are detected. Thus, the halogen–magnesium exchange reaction of **M3** was found to proceed exclusively at the 5-position to provide Grignard monomer **GM3a**. In contrast to our previous report,[21] only at the 5-position can the chloromagnesium group be stabilized by the intramolecular chelate coordination, which is the most likely reason for the regioselectivity of the halogen–magnesium exchange reaction. According to the integral ratio of the proton signals, the conversion of **M3** was calculated as 79%. The corresponding reaction of **M3** with *i*-PrMgCl under the same conditions exhibited a conversion of 78% and perfect regioselectivity, which suggests that the addition of LiCl does not influence the halogen–magnesium exchange reaction (Supplementary Figure S3).

Kumada coupling polymerization

After the regioselective halogen–magnesium exchange reaction of **M3** with *i*-PrMgCl·LiCl, the Kumada coupling polymerization of **GM3a** was performed using Ni(dppp)Cl$_2$ (3 mol%) in THF (Scheme 3). Because **GM3a** has a sterically hindered structure around the chloromagnesium group compared to 2-bromo-5-chloromagnesio-3-hexylthiophene, which is the typical Grignard monomer used for synthesizing P3HT, reflux temperature was required for the polymerization to proceed smoothly. Despite the presence of LiCl, similar to the case of **M2**, **GM3a** demonstrated low polymerization activity. The dark purple solid was precipitated on the surface of reaction flask as the polymerization progressed. The reaction was quenched with 1 M HCl solution after 24 h, and the organic phase was diluted with $CHCl_3$ and poured into hexane to isolate **P3′** as deep purple solid in 40% yield. The isolated **P3′** had relatively low solubility

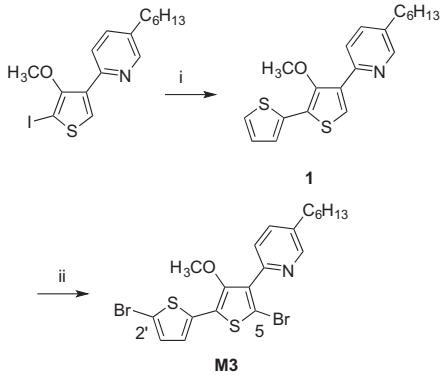

Scheme 1 Synthetic route for **M3**. (i) 2-tributylstannylthiophene, Pd(PPh3)4, toluene reflux, 3 days. (ii) NBS, THF/AcOH, room temperature, overnight.

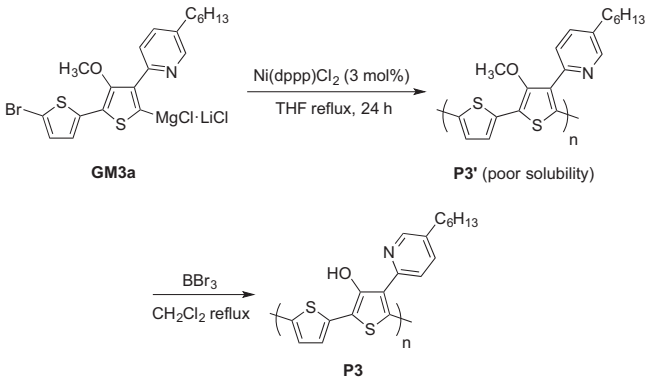

Scheme 3 Kumada coupling polymerization and intended polymer reaction.

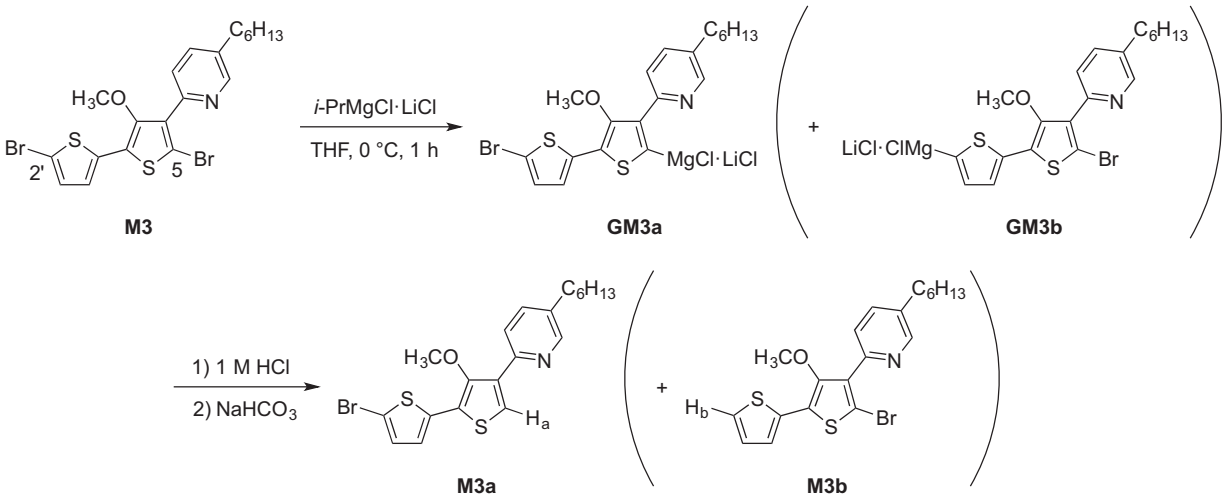

Scheme 2 Halogen–magnesium exchange reaction of **M3**.

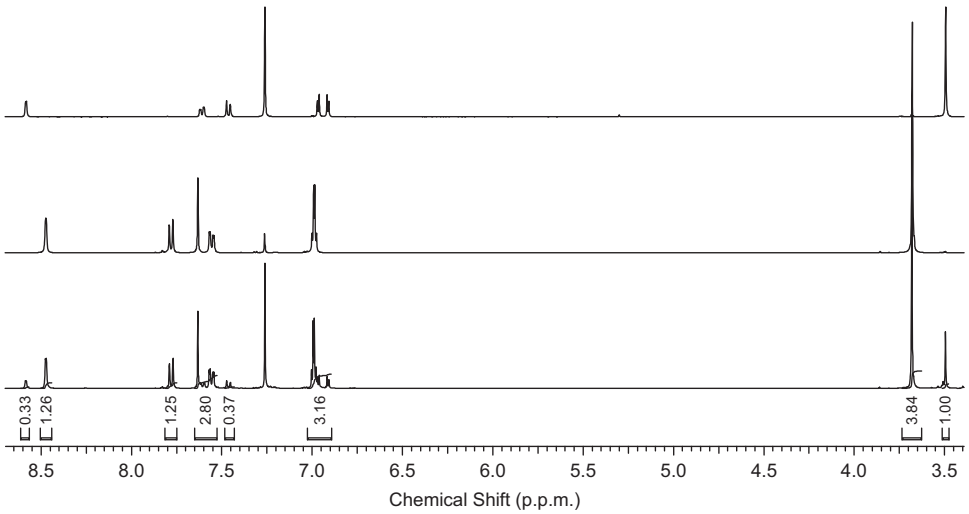

Figure 2 Expanded and stacked ^{1}H nuclear magnetic resonance spectra of **M3** (top), isolated **M3a** (middle) and the crude mixture from the halogen–magnesium exchange reaction using *i*-PrMgCl·LiCl (bottom).

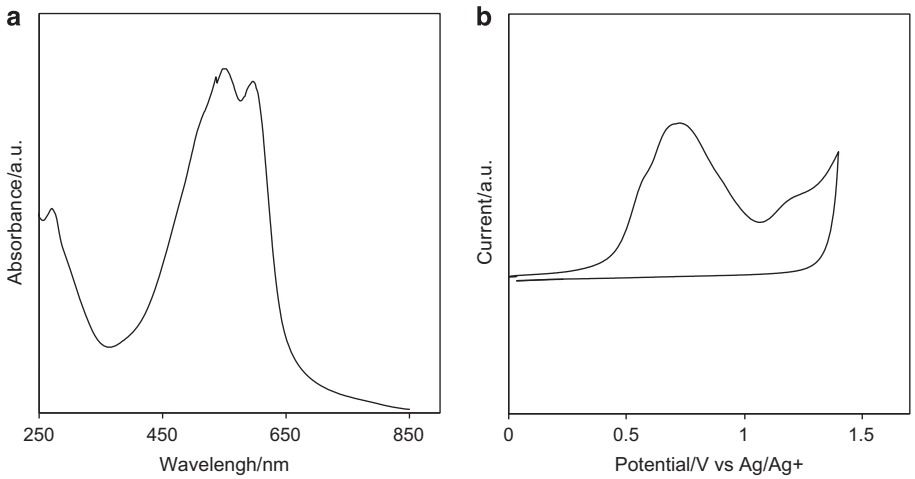

Figure 3 Ultraviolet–visible spectrum in 10^{-5} M $CHCl_3$ solution (**a**) and cyclic voltammogram in 0.1 M CH_3CN solution of tetrabutylammonium hexafluorophosphate (Bu_4NPF_6) (**b**) of **P3′**.

Table 1 HOMO, LUMO and E_g of P2′ and P3′

	HOMO (eV)[a]	*LUMO (eV)*[b]	E_g *(eV)*[c]
P2′	−5.27	−3.29	1.98
P3′	−5.17	−3.31	1.86

Abbreviations: HOMO, highest occupied molecular orbital; LUMO, lowest unoccupied molecular orbital.
[a]Determined from the oxidation onset potential (E_{onset}).
[b]LUMO = E_g+HOMO.
[c]Estimated from the onset wavelength of the absorption spectra.

in organic solvents such as $CHCl_3$, THF and toluene. The poor solubility of **P3′** prevented NMR characterization. **P3**, which can be obtained by treating **P3′** with BBr_3, is anticipated to have a much decreased solubility in comparison; therefore, we did not pursue the intended polymer reaction at this time. The poor solubility might be improved by introducing a branched long alkyl chain onto the pyridine ring, which will be examined in the future. The THF-soluble fraction of isolated **P3′** was analyzed by gel permeation chromatography, and the number-average molecular weight was estimated as $M_n = 2900$, which corresponds to a degree of polymerization of 8. The molecular weight distribution (M_w/M_n) was 1.4. The polymerization behavior was investigated using the ^{1}H-NMR spectrum of the hexane-soluble fraction shown in Supplementary Figure S4. As described above, the proton signals at 3.49 and 3.68 p.p.m. originate from unreacted **M3** and **M3a**, respectively. According to the nickel-catalyzed Kumada coupling polymerization mechanism proposed by Yokozawa *et al.*,[7] dibromo compound **M3** does not participate in the polymerization. Therefore, the conversion of **GM3a** was calculated as 72% by comparing the integral ratio of the methoxy proton signals in Figure 2 (3.84) with that in Supplementary Figure S4 (1.01). As a result, most of **P3′** was insoluble in $CHCl_3$ and THF, although the actual percentage of insoluble to soluble fraction was not determined. On the other hand, the Kumada coupling polymerization in the absence of LiCl exhibited a decreased monomer conversion as low as 15% (Supplementary Figure S5). This result is consistent with the finding of Geng *et al.*[23]

that the addition of LiCl promotes the polymerization of the sterically hindered 5-bromo-2-chloromagnesio-3-hexylthiophene (reverse monomer).

Optoelectronic properties

The UV–visible spectrum of **P3′** was collected in $CHCl_3$ solution (Figure 3a). The absorption maximum at 277 nm might originate from the repeating unit. The absorption maxima corresponding to the π–π^* transition band along the conjugated main chain were observed at 550 and 594 nm. These values exhibited a remarkable redshift from **P2′** without the thiophene spacer (476 nm; see Supplementary Figure S6 for the chemical structure).[21] This result likely stems from the planar conformation of **P3′**, although the regioregular derivative of **P2′** should be prepared to make an accurate comparison. The conformations of **P2′** and **P3′** were investigated by density functional theory calculations of the dimer model compounds. The ground-state structures of **P2′-dimer** and **P3′-dimer** were optimized at the B3LYP/6-31G(d) level of theory. As indicated in Supplementary Figure S6 and Supplementary Table S1, **P2′-dimer** had a dihedral angle of 116° between two thiophene rings, and no S···O interaction was observed, as determined by the intermolecular distance (3.47 Å) being longer than the sum of the van der Waals radii (3.32 Å). By contrast, for **P3′-dimer**, the average dihedral angle between four thiophene rings was 158°, indicating that **P3′** bearing the regiocontrolled head-to-tail structure adopts a more planar main chain conformation than **P2′**. Because the averaged S···O distance (2.95 Å) was shorter than the sum of the van der Waals radii, the planar conformation of **P3′** is likely due to the non-covalent S···O interaction.[24] In the spin-coated film, the absorption maxima exhibited a small redshift (558 and 601 nm) compared to those in solution. Although X-ray diffraction experiments are necessary for a detailed discussion, this redshift indicates that **P3′** does not form an effective π–π stacking structure in the solid state. The electrochemical properties of **P3′** were investigated by measuring the cyclic voltammogram of the polymer film on a platinum electrode in 0.1 M CH_3CN solution of tetrabutylammonium hexafluorophosphate (Bu_4NPF_6) (Figure 3b). In the anodic scan, an irreversible oxidation peak with a maximum at 0.7 V was observed. On the basis of the onset potential, the HOMO energy level was calculated as −5.17 eV using the following equation: HOMO = −(E_{onset}+4.73) eV, where the energy level is calibrated against the ferrocene/ferrocenium couple (Fc/Fc^+ measured as 0.07 V vs Ag/Ag^+) and 4.8 eV is the energy level of Fc under vacuum. The HOMO energy level of **P3′** was therefore higher than that of **P2′** (−5.27 eV), reflecting the presence of the electron-rich thiophene ring. The LUMO energy level of **P3′** was estimated as −3.31 eV from the HOMO energy level and the optical bandgap energy (E_g) in the UV–visible absorption spectrum. Time-dependent density functional theory calculations were performed for **P2′-dimer** and **P3′-dimer** at the B3LYP/6-31G(d) level of theory. The vertical one-electron excitations with the largest oscillator strength were from the HOMO to the LUMO in both cases, and the bandgap energy of **P3′-dimer** was clearly decreased compared with that of **P2′-dimer** (Supplementary Figure S7). For **P3′-dimer**, the HOMO surface was distributed over the whole oligo(thiophene) moiety, and the LUMO surface was relatively localized on the pyridine moiety. Thus, the theoretical time-dependent density functional theory calculations qualitatively account for the optoelectronic properties of **P2′** and **P3′**, although there are some discrepancies between the calculated and experimental values (Table 1).

CONCLUSIONS

New dibromobithiophene monomer **M3** featuring pyridine and methoxy groups at the β-position was prepared from a known thiophene compound via the Stille coupling reaction followed by bromination. The halogen–magnesium exchange reaction of **M3** with *i*-PrMgCl·LiCl occurred exclusively at the bromine atom neighboring the pyridine group. The Kumada coupling polymerization of *in situ*-generated Grignard monomer **GM3a** using $Ni(dppp)Cl_2$ proceeded smoothly at reflux temperature in the presence of LiCl. Because of the poor solubility, the number-average molecular weight of oligo(bithiophene) **P3′** with the regiocontrolled structure remained low. The UV–visible and cyclic voltammogram measurements along with the theoretical density functional theory calculations suggested that **P3′** had a more planar conformation and narrower bandgap energy than our previously reported polythiophene derivative due to a non-covalent S···O interaction.

CONFLICT OF INTEREST

The authors declare no conflict of interest.

ACKNOWLEDGEMENTS

This work was supported by the JSPS KAKENHI Grant-in-Aid for Scientific Research (C) 23550135, NAGAI Foundation for Science & Technology and Ogasawara Foundation for the Promotion of Science & Engineering.

1 Kim, Y., Cook, S., Tuladhsr, S. M., Choulis, S. A., Nelson, J., Durrunt, J. R., Bradkey, D. D. C., Giles, M., McCulloch, I., Ha, C. S. & Ree, M. A strong regioregularity effect in self-organizing conjugated polymer films and high-efficiency polythiophene: fullerene solar cells. *Nat. Mater.* **5**, 197–203 (2006).
2 Allard, S., Forster, M., Souharce, B., Thiem, H. & Scherf, U. Organic semiconductors for solution-processable field-effect transistors (OFETs). *Angew. Chem. Int. Ed.* **47**, 4070–4098 (2008).
3 McCullough, R. D. & Lowe, R. D. Enhanced electrical conductivity in regioselectively synthesized poly(3-alkylthiophenes). *J. Chem. Soc. Chem. Commun.* 70–72 (1992).
4 Sheina, E. E., Liu, J., Iovu, M. C., Laird, D. W. & McCullough, R. D. Chain growth mechanism for regioregular nickel-initiated cross-coupling polymerizations. *Macromolecules* **37**, 3526–3528 (2004).
5 Robert, S. L., Paul, C. E., Jinsong, L., Lei, Z. & McCullough, R. D. Regioregular, head-to-tail coupled poly(3-alkylthiophenes) made easy by the GRIM method: investigation of the reaction and the origin of regioselectivity. *Macromolecules* **34**, 4324–4333 (2001).
6 Yokoyama, A., Miyakoshi, R. & Yokozawa, T. Chain-growth polymerization for poly(3-hexylthiophene) with a defined molecular weight and a low polydispersity. *Macromolecules* **37**, 1169–1171 (2004).
7 Yokoyama, A., Miyakoshi, R. & Yokozawa, T. Catalyst-transfer polycondensation. mechanism of Ni-catalyzed chain-growth polymerization leading to well-defined poly (3-hexylthiophene). *J. Am. Chem. Soc.* **127**, 17542–17547 (2005).
8 Peeters, H., Jivanescu, M., Stesmans, A., Pereira, L., Dillemans, L. & Koeckelberghs, G. Influence of the bulkiness of the substituent on the aggregation and magnetic properties of poly(3-alkylthiophene)s. *J. Polym. Sci. A Polym. Chem.* **52**, 76–86 (2014).
9 Khlyabich, P. P., Rudenko, A. E. & Thompson, B. C. Random poly(3-hexylthiophene-co-3-cyanothiophene) copolymers with high open-circuit voltage in organic solar cells. *J. Polym. Sci. A Polym. Chem.* **52**, 1055–1058 (2014).
10 Noh, S., Gobalasingham, N. S. & Thompson, B. C. Facile enhancement of open-circuit voltage in P3HT analogues via incorporation of hexyl thiophene-3-carboxylate. *Macromolecules* **49**, 6835–6845 (2016).
11 Xu, M.-H. & Pu, L. Novel unsymmetrically hyperbranched polythiophenes with conjugation gradient. *Tetrahedron Lett.* **43**, 6347–6350 (2002).
12 Okamoto, K., Housekeeper, J. B., Michael, F. E. & Luscombe, C. K. Thiophene based hyperbranched polymers with tunable branching using direct arylation methods. *Polym. Chem.* **4**, 3499–3506 (2013).
13 Murakami, K., Tanaka, S. & Mori, A. Linear-selective cross-coupling polymerization of branched oligothiophene by deprotonative metalation and cross-coupling. *Polym. Chem.* **6**, 6573–6578 (2015).
14 Holcombe, T. W., Woo, C. H., Kavulak, D. F. J., Thompson, B. C. & Fréchet, J. M. J. All-polymer photovoltaic devices of poly(3-(4-*n*-octyl)-phenylthiophene) from Grignard metathesis (GRIM) polymerization. *J. Am. Chem. Soc.* **131**, 14160–14161 (2009).

15 Ohshimizu, K., Takahashi, A., Rho, Y., Higashihara, T., Ree, M. & Ueda, M. Synthesis and characterization of polythiophenes bearing aromatic groups at the 3-position. *Macromolecules* **44**, 719–727 (2011).
16 Lai, Y.-C., Ohshimizu, K., Takahashi, A., Hsu, J.-C., Higashihara, T., Ueda, M. & Chen, W.-C. Synthesis of all-conjugated poly(3-hexylthiophene)-block-poly(3-(4′-(3″,7″-dimethyloctyloxy)-3′-pyridinyl)thiophene) and its blend for photovoltaic applications. *J. Polym. Sci. A Polym. Chem.* **49**, 2577–2587 (2011).
17 Richter, T. V., Braun, C. H., Link, S., Scheuble, M., Crossland, E. J. W., Stelzl, F., Würfel, U. & Ludwigs, S. Regioregular polythiophenes with alkylthiophene side chains. *Macromolecules* **45**, 5782–5788 (2012).
18 Ouhib, F., Hiorns, R. C., Bettignies, R., Bailly, S., Desbrières, J. & Dagron-Lartigau, C. Photovoltaic cells based on polythiophenes carrying lateral phenyl groups. *Thin Solid Films* **516**, 7199–7204 (2008).
19 Takagi, K., Joo, H., Yamashita, Y., Kawagita, E. & Torii, C. Regioselective Grignard metathesis reaction of 2,5-dibromo-3-(6′-hexylpyridine-2′-yl)thiophene and Kumada coupling polymerization. *J. Polym. Sci. A Polym. Chem.* **49**, 4013–4020 (2011).
20 Takagi, K., Kawagita, E. & Kouchi, R. Synthesis and characterization of polythiophene derivatives with nitrogen heterocycles on the side chain. *J. Polym. Sci. A Polym. Chem.* **52**, 2166–2174 (2014).
21 Takagi, K., Kouchi, R. & Kawai, J. Synthesis of polythiophene derivative bearing methoxy and pyridine groups at the b-position and formation of an intramolecular hydrogen bonding through the polymer reaction. *Polymer* **114**, 221–230 (2017).
22 Koeckelberghs, G., Vangheluwe, M., Doorsselaere, K. V., Robijns, E., Persoons, A. & Verbiest, T. Regioregularity in poly(3-alkoxythiophene)s: effects on the faraday rotation and polymerization mechanism. *Macromol. Rapid Commun.* **27**, 1920–1925 (2006).
23 Wu, S., Huang, L., Tian, H., Geng, Y. & Wang, F. LiCl-promoted chain growth Kumada catalyst-transfer polycondensation of the 'reversed' thiophene monomer. *Macromolecules* **44**, 7558–7567 (2011).
24 Guo, X., Quinn, J., Chen, Z., Usta, H., Zheng, Y., Xia, Y., Hennek, J. M., Ortiz, R. P., Marks, T. J. & Facchetti, A. Dialkoxybithiazole: a new building block for head-to-head polymer semiconductors. *J. Am. Chem. Soc.* **135**, 1986–1996 (2013).

Supplementary Information accompanies the paper on Polymer Journal website (http://www.nature.com/pj)